Generation and control of hot spots on commensurate metallic gratings

Aude Barbara, Jérôme Le Perchec, Stéphane Collin, Christophe Sauvan, Jean-Luc Pelouard, Tomas Lopez-Rios, Pascal Quemerais

Generation and control of hot spots on commensurate metallic gratings

A. Barbara,[1] J. Le Perchec,[1] S. Collin,[2] C. Sauvan,[2] J-L. Pelouard,[2] T. López-Ríos,[1] and P. Quémerais[1]

[1]*Institut Néel, CNRS et Universit Joseph Fourier, BP 166, F-38042 Grenoble Cedex 9, France*

[2]*Laboratoire de Photonique et Nanostructures (LPN/CNRS), Route de Nozay, 91460 Marcoussis, France*

aude.barbara@grenoble.cnrs.fr

Abstract: We study the light localization on commensurate arrangements of deep metallic sub-wavelength grooves. We theoretically show that as the degree of commensuration tends to an irrational number new light localization states are produced. These have properties close to that reported for hot spots on disordered surfaces and are not permitted for simple period gratings. Existence of these new resonances is experimentally provided in the infra-red region by reflectivity measurements performed on two commensurate samples with respectively two and three slits per period. Manipulations of these hot spots which can be controlled from far-field could be used for high sensitivity spectroscopy applications.

OCIS codes: (260.3910) Metal optics; (240.6680) Surface plasmons; (240.6695) Surface-enhanced Raman scattering; (050.6624) Subwavelength structures.

References and links

1. E. Albano, S. Daiser, G. Ertl, R. Miranda, K. Wandelt and N. Garcia, "Nature of surface-enhanced-Raman-scattering active sites on coldly condensed Ag films," Phys. Rev. Lett. **51,** 2314-2317 (1983).
2. A. Hessel and A. A. Oliner, "Wood's anomaly effects on gratings of large amplitude," Opt. Commun. **59,** 327 (1986).
3. A. Wirgin and T. López-Ríos, "Can surface enhanced Raman scattering be caused by waveguide resonances?," Opt. Commun. **48,** 416-420 (1984) and T. Lopez-Rios and A. Wirgin Opt. Commun. **49,** 455 (1984).(errata)
4. A. Wirgin, A.A. Maradudin, "Resonant response of a bare metallic grating to s-polarized light," Prog. Surf. Sci. **22,** 1 (1986).
5. G. Tayeb and R. Petit, "On the numerical study of deep conducting lamellar diffraction gratings," Opt. Acta **31(12,)** 1361 (1984).
6. M. Sobnack, W. Tan, N. Wanstall, T. Preist and R. Sambles, "Stationary surface plasmons on zero-order metal grating," Phys. Rev. Lett. **80,** 5667 (1998).
7. T. López-Ríos, D. Mendoza, FJ. García-Vidal, J. Sánchez-Dehesa and B. Pannetier, "Surface shape resonances in lamellar metallic gratings," Phys. Rev. Lett. **81,** 665 (1998).
8. D. Crouse, "Numerical modeling and electromagnetic resonant modes in complex grating structures and opto-electronic device applications," IEEE Trans. Electron. Dev. **52(11),** 2365 (2005).
9. C. Douketis, Z. Wang, T.L. Haslett and M. Moskovits, "Fractal character of cold-deposited silver films determined by low-temperature scanning tunneling microscopy," Phys. Rev. B **51,** 11022-11031 (1995).
10. J. Le Perchec, P. Quémerais, A. Barbara and T. López-Ríos, "Why metallic surfaces with grooves a few nanometers deep and wide may strongly absorb visible light," Phys. Rev. Lett. **100,** 066408 (2008).
11. S. Grésillon, L. Aigouy, A. Boccara, J. C. Rivoal, X. Quelin, C. Desmarest and P. Gadenne, "Experimental Observation of Localized Excitations in Random Metal-Dielectric Films," Phys. Rev. Lett **82,** 4520 (1999).
12. S. Ducourtieux, V. Podolskiy, S. Grésillon, S. Buil, B. Berini, P. Gadenne, A. Boccara, JC Rivoal, W. Bragg, K. Banerjee, V. Safonov, V. Drachev, Z. Ying, A. Sarychev and V. Shalaev, "Near-field optical studies of semicontinous metal films," Phys. Rev. B **64,** 165403 (2001).

#102049 - $15.00 USD Received 26 Sep 2008; revised 7 Oct 2008; accepted 12 Oct 2008; published 4 Nov 2008

13. C. Berger, E. Belin, D. Mayou, "Electronic properties of quasicrystals," Ann. Chimi. Mater. (Paris) **18,** 485 (1993).
14. E. Belin, D. Mayou,"Electronic properties of quasicrystals," Phys. Scr. **T49,** 356 (1993).
15. G. Trambly de Lassardiére, D. Nguyen-Manh, D. Mayou,"Electronic structure of complex Hume-Rothery phases and quasicrystals in transition metal aluminides," Prog. Mater. Sci. **50,** 679 (2005).
16. S. Aubry and P. Quémerais in Low-dimensional electronic properties of Molybdenum bronzes and oxides, p.293 (Ed. C. Schlenker, Kluwer Academic publishers 1989).
17. D. Skigin and R. Depine, "Transmission Resonances of Metallic Compound Gratings with Subwavelength Slits," Phys. Rev. lett. **95,** 217402 (2005) and references therein.
18. T. Matsui, A. Agrawal, A. Nahata and Z.V. Vardeny, "Transmission resonances through aperiodic arrays of subwavelength apertures," Nature **446,** 517 (2007).
19. A. Hibbins, I. Hooper, M. Lockyear and R. Sambles, "Microwave transmission of a compound metal grating," Phys. Rev. Lett. **96,** 257402 (2006).
20. H. A. Rowland, Phys. papers, Johns Hopkins Univ. Press, Baltimore (1902).
21. F. Ducastelle and P. Quémerais, "Chemical Self-Organization During Crystal Growth," Phys. Rev. Lett. **78,** 102 (1997).
22. F. Ducastelle, "Order and phase stability in alloys," Cohesion and Structure vol. 3, (Ed. F.R. De Boer, D. G. Pettifor, North-Holland 1991).
23. E. D. Palik, *Handbook of Optical Constants of Solids*, Academic Press.
24. J. Le Perchec, P. Quémerais, A. Barbara and T. López-Ríos, "Controlling Strong Electromagnetic Fields at Subwavelength Scales," Phys. Rev. Lett. **97,** 036405 (2006).
25. P. Zhang, T.L. Haslett, C. Douketis and M. Moskovits, "Mode localization in self-affine fractal interfaces observed by near-field microscopy," Phys. Rev. B **57,** 15513 (1998).
26. H. P. Lu, "Site-specific Raman spectroscopy and chemical dynamics of nanscale intersticial systems," J. Phys: Condens. Matter. **17,** R333 (2005).
27. A. Barbara, P. Quémerais, E. Bustarret, T. López-Ríos and T. Fournier, "Electromagnetic resonances of subwavelength rectangular metallic gratings,"Eur. Phys. J. D. **23,** 143-154 (2003).
28. A. Barbara, P. Quémerais, E. Bustarret and T. López-Ríos, "Optical transmission through subwavelength metallic gratings," Phys. Rev B. **66,** 161403(R) (2002).
29. A. Barbara, J. Le Perchec, P. Quémerais and T. López-Ríos, "Experimental evidence of efficient cavity modes excitation in metallic gratings by attenuated total reflection," J. Appl. Phys. **98,** 033705 (2005).
30. S. Collin, F. Pardo, R. Teissier and J-L Pelouard, "Efficient light absorption in metalsemiconductormetal nanostructures," Appl. Phys. Lett **85,** 194 (2004).
31. C. Billaudeau, S. Collin, C. Sauvan, N. Bardou, F. Pardo and J-L Pelouard, "Angle-resolved transmission measurements through anisotropic 2D plasmonic crystals," Opt. Lett. **33,** 165 (2008).

1. Introduction

Interaction between light and metallic structures may lead to local near field enhancements known as hot spots. They are due to light localization and may be associated with far-field intriguing properties such as the abnormal optical absorption or the Surface Enhanced Raman Scattering (SERS) effect. Among the various metallic surfaces supporting hot spots, subwavelength metallic gratings with deep rectangular grooves are known to be model systems for studying the light trapping due to the excitation of surface plasmons polaritons. Historically, an outstanding experiment made by Albano et al.[1] first showed the prominent role of deep crevasses on metallic surfaces to generate surface enhancement Raman scattering (SERS), which is itself directly related to local field enhancements. Since this experiment, cavity modes in gratings were extensively studied[2, 3, 4, 5, 6, 7, 8]. This approach gave much insight of the physics involved but quantitative understanding of important experimental facts observed of randomly rough surfaces remained unexplained. Firstly, nanoscale roughnesses[1, 9] could present strong near-field enhancements and light absorption in the visible spectral range that were only recently understood[10] : grooves with nanometric size may indeed resonate in the visible range when quasi-static surface plasmon resonances are excited inside the grooves. The optical excitation of these quasi-static plasmons also permits to produce field enhancement thousands times larger than the impinging light, in accordance with experimentally observed SERS enhancements which are usually not correctly restituted by the calculations. The second general experimental point concerns the existence of hot spots and the possible localization

#102049 - $15.00 USD Received 26 Sep 2008; revised 7 Oct 2008; accepted 12 Oct 2008; published 4 Nov 2008

of light by disorder[11]. One puzzling point is that the light localization properties are highly sensitive to external parameters[12]: a small change (only a few percents) of the exciting wavelength may lead to an important geometrical reorganization of the hot spots.
In the present paper we show that we can generate and control wavelength-dependant hot spots from far-field considering ordered surfaces which can be experimentally and theoretically controlled. We study the influence of the commensurate arrangement of subwavelength deep metallic grooves on the light localization. We do know from solid state physics that incommensurate structures, such as quasi-crystals for instance, and commensurate approximates may present particular electron localization states forbidden for purely periodic systems[13, 14, 15, 16]. New light localization phenomena can thus be expected by merging electromagnetic resonances of deep metallic grooves and one-dimensional commensurate structures. Far-field transmission through slits arrays with N grooves per period separated by the same distance or through aperiodic 2-dimension hole arrays have reported on the existence of sharp transmission resonances due to modification of the short-range order[17, 18, 19]. Using the formalism of commensurate structures we have built and studied the optical properties of metallic surfaces of successive commensurate structures with increasing periods and followed their behaviour from the simplest case of a simple-periodic grating to an almost aperiodic one. We show that new strong and sharp electromagnetic resonances associated to light localization states forbidden for purely period system indeed appear. They are very localized and the near-field enhancements inside the grooves is wavelength-dependent. In far-field these resonances are evidenced by sharp dips in the reflectivity which remind of Rowland's "ghost" lines observed in the diffraction for gratings presenting periodic defaults in their spacings[20]. Finally, we give the first experimental proof of their existence in the infra-red region for gratings with respectively two and three slits per period.

2. Calculated optical response of the commensurate structures

2.1. Presentation of the commensurate structures

An example of the arrangements that we study is sketched in Fig.1. They are gratings composed of several identical closed rectangular deep grooves per period separated by two possible subwavelength distances L (for long distance) and S (for short distance). The number of grooves separated by the distance S is noted R while Q denotes for the total number of grooves within a period. Consequently these commensurate structures are called R/Q gratings, their period is $D = R \times S + (Q-R) \times L$ and the ratio R/Q indicating the order of commensurability is chosen to be an irreducible rational number. When R/Q tends to any irrational number, the structure tends to an aperiodic (or incommensurate) one[21] with $D \rightarrow \infty$. The successive sequences of ratios R/Q is chosen to be uniform[16, 22, 21] and permits to build a succession of approximating periodic structures progressively tending to an aperiodic one. In the present work we consider the successive R/Q ratios built by using the Fibonacci series $\{1,2,3,5,8,13...\}$ giving the ratios $\{<1/2>,<2/3>,<3/5>,<5/8>...\}$. for which R/Q tends to $\xi = (\sqrt{5}-1)/2$ the inverse of the mean gold number at large values of R and Q. Any other irrational number than ξ would also lead to an aperiodic structure. Systems with N grooves per period separated by the same distance were theoretically studied[17]. They correspond to $SSS..(\times R)L$ arrangements and up to three cavities per period they are equivalent to the present commensurate structures but as grooves continue to be added both their near and far field properties become very different since our structures tend to aperiodic systems and not to periodic ones.

2.2. The modal method for commensurate gratings

We have calculated the optical response of the commensurate gratings illuminated by a p-polarized plane wave (magnetic field parallel to the groove) by using an approximated modal

#102049 - $15.00 USD Received 26 Sep 2008; revised 7 Oct 2008; accepted 12 Oct 2008; published 4 Nov 2008

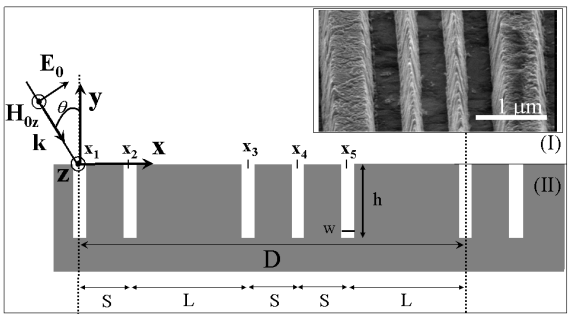

Fig. 1. Example of a uniformly ordered commensurate structure $< 3/5 >$ of period $D = 3S + 2L$ where L and S respectively stand for the long and short distances separating two cavities. The grooves are identical with an aperture w and a height h. Inset represents a SEM image of the $< 2/3 >$ gold sample.

method based on the surface impedance boundary conditions[4]. The latter has been several times successfully compared with experiments[28, 29] when considering gold gratings with sub-micron geometrical parameters in the infra-red region as it is the case here. In this method the magnetic field is first expressed in the region (I) above the grating (Fig.1) by the Rayleigh development:

$$H_z^{(I)}(x,y) = e^{ik(\gamma_0 x - \beta_0 y)} + \sum_{m=-\infty}^{m=+\infty} R_m e^{ik(\gamma_m x + \beta_m y)},$$

where $k = 2\pi/\lambda$ is the wave vector of the incident plane wave. The terms $\gamma_m = sin\theta + m\lambda/D$, $\beta_m^2 = 1 - \gamma_m^2$ and R_m are respectively the normalized wave vectors and the amplitude of the m^{th} order of reflection.

In the region (II) of the grating the field is expressed inside each cavity of the period by applying the surface impedance approximation at the bottom of the cavity and considering the vertical walls as perfectly conducting:

$$\begin{aligned} H_z^{(II)}(x,y) &= \sum_{p=1}^{Q} \sum_{n=0}^{+\infty} A_p^n \cos\left[\frac{n\pi}{w}\left(x - x_p + \frac{w}{2}\right)\right] \\ &\times \left(e^{i\mu_n(y+2h)} + r_n e^{-i\mu_n y}\right) \sqcap (x - x_p) \end{aligned} \quad (1)$$

where A_p^n is the amplitude of the n^{th} mode in the p^{th} cavity whose vertical component of the wave vector is $\mu_n = k\sqrt{1 - (\frac{n\lambda}{2w})^2}$. The coefficients $r_n = (\mu_n/k + Z)/(\mu_n/k - Z)$, where $Z = 1/\sqrt{\varepsilon}$ and ε the dielectric constant of the metal, are the reflection coefficients of the n^{th} mode at the bottom of the cavity. $\sqcap(x - x_p) = 1$ for $(x - x_p) \in [-w/2, w/2]$ and 0 elsewhere. $\{x_p\}_{1 \le p \le Q}$ is a series of the location of the center of the Q cavities contained in a period. The origin is $x_1 = 0$ and the other locations are determined using the equation[21]:

$$\begin{aligned} x_{p+1} &= x_p + S \times \sigma_p + L \times (1 - \sigma_p) \\ with \quad \sigma_p &= [p \times R/Q] - [(p-1) \times R/Q] \end{aligned}$$

where the function $[y]$ defines the integer part of y and p the number of the cavity.

From the expression of the fields in both regions and following the procedure detailed in ref[27] one can determine all the coefficients A_p^n and R_n which enable to know the electromagnetic field in the whole space.

#102049 - $15.00 USD Received 26 Sep 2008; revised 7 Oct 2008; accepted 12 Oct 2008; published 4 Nov 2008

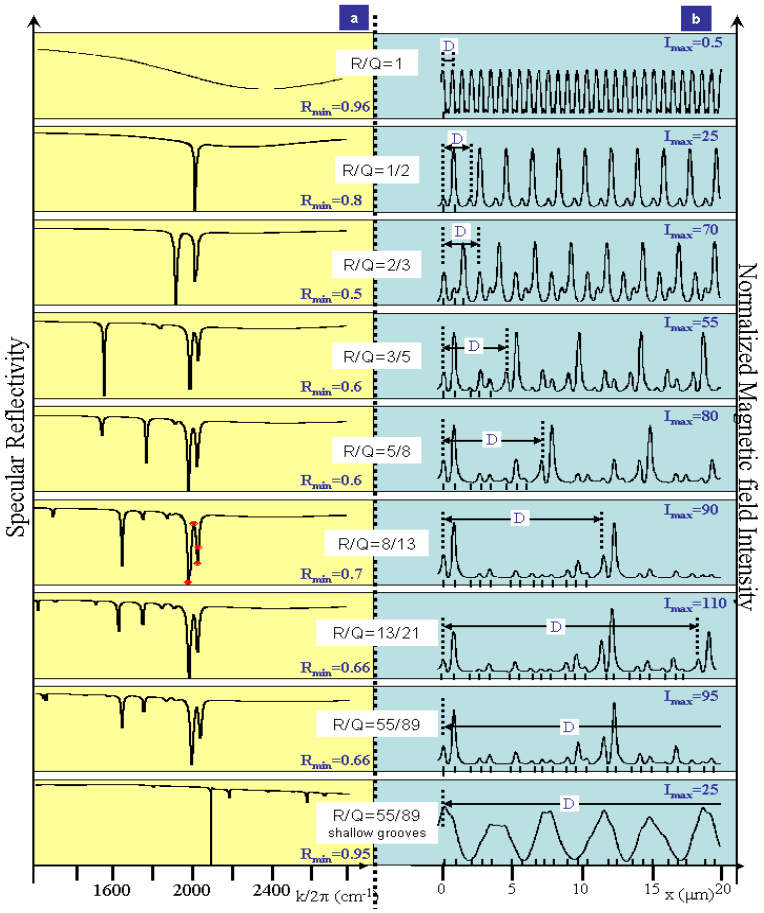

Fig. 2. (Color Online)(a) Calculated specular reflectivity as R/Q tends to the inverse of the mean golden number and (b) magnetic near-field intensity at the interface $y = 0$ at the frequency resonance located around 2000 cm^{-1} where the reflectivity is minimal. Y-scale goes from R_{min} to 1 in (a) and from 0 to I_{Max} in (b). Simulations were made considering $w = 0.3\mu m$, $S = 0.7\mu m$, $L = 1.2\mu m$, $h = 1\mu m$, and an incidence angle $\theta = 15°$. Vertical black lines in (b) indicate the position of the cavities within one period. For shallow grooves ($h = 0.2\mu m$) the strong resonances disappear. Only weak resonances due to the horizontal surface plasmon subsist and the near-field exhibits no hot spots.

2.3. *Numerical results and discussion*

Figure 2(a) displays the evolution of the specular reflectivity calculated at $\theta = 15\,^{\circ}$ as the order of commensurability tends to ξ and starts from a purely periodic grating. Simulations were made using the gold dielectric constant from ref[23] and considering only the fundamental guided mode since $w << \lambda$ (n=0 in eq.1). For a simple-period grating $R/Q = 1$ the spectrum presents the well-known broad dip due to the excitation of the Fabry-Perot like resonance inside the cavities[7] and as grooves are added supplementary and sharp resonances appear. These resonances are related to the Fabry-Perot like cavity modes and disappear for shallow grooves. In that case, only weak resonances due to the horizontal surface plasmon (SP) persist. In the spectral range and the geometrical parameters we consider here, the SP of the horizontal interface play a minor role. For large Q values (here $Q > 8$) only slight changes appear from

#102049 - $15.00 USD Received 26 Sep 2008; revised 7 Oct 2008; accepted 12 Oct 2008; published 4 Nov 2008

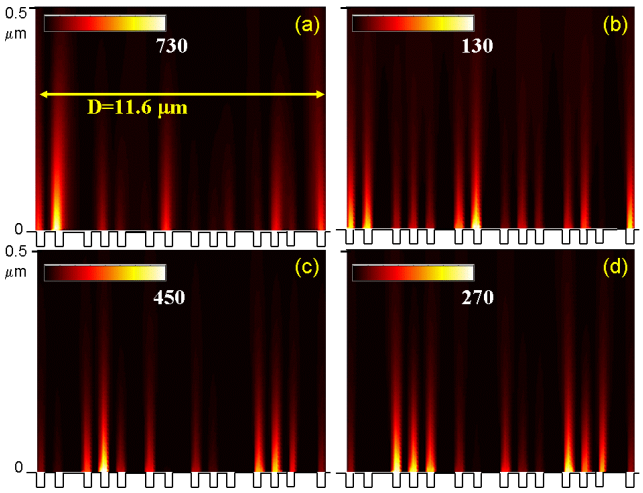

Fig. 3. (Color Online) Intensity maps of the electric field along the x-axis above one period of the $< 8/13 >$ grating considered on Fig.2. Calculations were made at the frequencies indicated by green dots on Fig.2(a): (a) 1985 cm^{-1}, (b) 2015 cm^{-1},(c) 2035 cm^{-1} and (d) 2040 cm^{-1}.The fluctuation of the photons localization is clearly illustrated, while the incident wave number varies by only a few percent.

one structure to the next one: the optical properties converge. This is a direct indication of the self-similarity of the structures produced as $R/Q \rightarrow \xi$ by using the standard Diophantine approximation [22, 16, 21] and ensures the accuracy of the numerical results. Fig.2b shows the simultaneously progressive establishment of hot spots at the surface as $R/Q \rightarrow \xi$. In the chosen configuration, the magnetic field intensity at the interface can locally be more than two orders of magnitude larger than the incident one (Fig.2(b)) and this corresponds to enhancements of the electric field intensity at the interface, larger than three orders of magnitude. Calculations were made at the frequency resonance around 2000 cm^{-1} corresponding to the strongest deep in the reflectivity spectra.

The occurrence of these new sharp cavity modes is due to the breaking of symmetry of the system. The pseudo-periodicity of the fields remains valid for the global period D so that cavities within a period do not see the same exciting field. A physical image can be given by analogy with coupled dipoles. In fact, in the case of a two-groove system a complete analytical study of the field expression can be performed and permits to characterize the nature of the resonances quantitatively[24]: each resonating cavity acts as a damped oscillating dipole and their near-field coupling causes the splitting of each individual mode into a large one corresponding to the symmetric coupling of the cavities ($\rightarrow\rightarrow$) and a thin one, corresponding to the anti-symmetric coupling ($\rightarrow\leftarrow$). In the same manner, in R/Q arrangements, the Q resonating cavities act as Q oscillating coupled dipoles, each mode corresponding to a specific configuration of the orientation of the dipoles. Depending on the number of dipoles oscillating in phase or out of phase, the mode will be more or less radiative. The less radiative the mode is, the narrowest the resonance is and the more intense the near-field enhancements is. Even though the Q cavities are identical they still resonate at slightly different frequencies. Consequently, the local intensity enhancements can be quite critically wavelength-dependent. This property of spectral fluctuation of the hot spots at nanoscale sites is experimentally observed on disordered surfaces[12], self-affine films[25] or SERS active surfaces[26]. This point is illustrated in Fig. 3 which represents maps of the electric field intensity along the x-axis and above a unit cell of the $< 8/13 >$

#102049 - $15.00 USD Received 26 Sep 2008; revised 7 Oct 2008; accepted 12 Oct 2008; published 4 Nov 2008

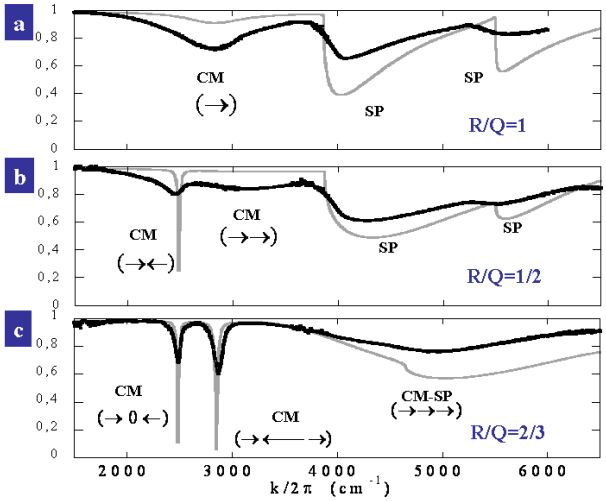

Fig. 4. (Color Online) Measured (black) and calculated (gray) specular reflectivity at $\theta = 10^\circ$ of the gratings $< 1/1 >$ (a), $< 1/2 >$ (b) and $< 2/3 >$ (c). Cavity resonances are noted CM and surface plasmon SP. The arrows indicate the direction of the equivalent dipole momentum at the mouth of each cavity.

grating calculated at different incident wave-numbers (red dots in Fig. 2(a)). Within a very narrow spectral range, here $55 cm^{-1}$, the spatial localization of the electromagnetic field is strongly modified. For specific frequencies, only a few cavities act as active sites by almost individually concentrating a great amount of energy whereas the neighboring ones are extinguished (Fig. 3(a) and 3(c)). For a single groove per period, all the cavities would localize the same amount of electromagnetic field over a spectral range of the order of $500 - 1000\ cm^{-1}$.

3. Experimental validation

The first step toward the validation of these theoretical predictions was to evidence the splitting of the cavity mode via the measurement of the new sharp resonances in the reflectivity spectra. Commensurate gratings with one, two and three slits per period and respective period $D_{<1/1>} = 2.2\mu m$, $D_{<1/2>} = 2.2\mu m$ ($L = 1.5\mu m$, $S = 0.7\mu m$) and $D_{<2/3>} = 2.6\mu m$ ($L = 1.2\mu m$, $S = 0.7\mu m$) were fabricated. They were prepared by electron-beam lithography and a double lift-off technique described in ref.[30, 31]: A Si substrate is first covered with a 200 nm-thick gold layer and secondly with a 1 μm-thick Si_3N_4 layer deposited by plasma-enhanced chemical vapor deposition. Si_3N_4 walls of the width of the slits and separated either by the distance L or S, are performed by electron-beam lithography and reactive ionic etching. A 650 nm-thick gold layer is then deposited, and the Si_3N_4 walls are lifted-off by means of a HF solution. The total area of the gratings is $2 \times 2\ mm^2$. SEM images show that the obtained grooves have a trapezoidal shape ($w_{down} = 0.3 - 0.36\mu m$ and $w_{top} = 0.5 - 0.62\mu m$) and that the metallic strip in-between two close cavities may become very narrow at the top (inset fig.1). Reflectivity measurements of p-polarized impinging light were performed at room temperature, in dry air, in the 1.67 to 6 μm spectral range, with a BioRad FTS60A DigiLab Fourier Transform photospectrometer. Spectra were normalized to the reflectivity of a flat gold surface. Figure 4 shows the specular reflectivity measured at $\theta = 10^\circ$ and the calculated spectra. In fig 4a, one can see the large cavity mode (CM) of the $< 1/1 >$ grating as well as the $n = \pm 1$ branches of the surface plasmons (SP)[27]. These SP occur around the same wave number for

#102049 - $15.00 USD Received 26 Sep 2008; revised 7 Oct 2008; accepted 12 Oct 2008; published 4 Nov 2008

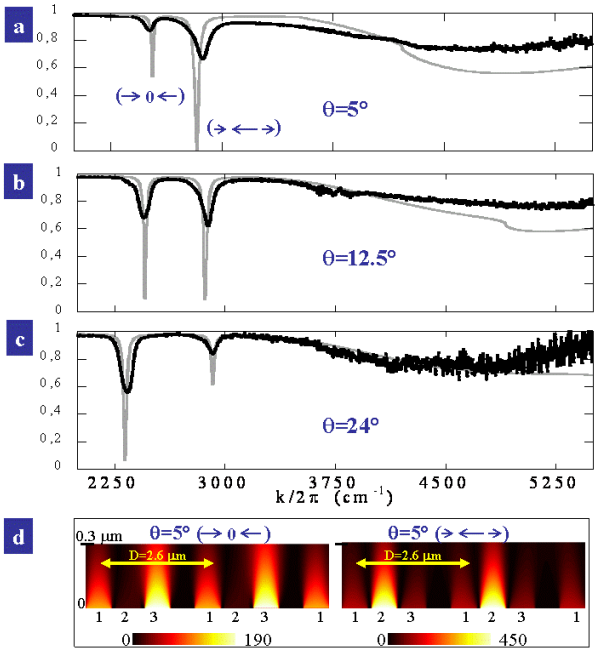

Fig. 5. (Color Online) Experimental (black) and calculated (gray) turnover of the relative reflectivity minima of the two sharp resonances for the $< 2/3 >$ grating when varying the incidence angle $\theta = 5°$ (a), $\theta = 12.5°$ (b), $\theta = 24°$ (c). (d) displays maps of the near-electric field intensity along the x-axis and above the cavities for to the antisymmetric (left) and symmetric (right) resonances measured at $\theta = 5°$.

the two other gratings since the period of the three samples have close values. More interestingly, we observe the splitting of the large CM into the new resonances predicted by our model. The $< 1/2 >$ grating presents the in-phase large cavity resonance together with a sharper resonance corresponding to the out-of phase coupling of the two cavities while the $< 2/3 >$ grating exhibits two sharp resonances together with the large cavity mode. The three resonances of $< 2/3 >$ correspond to:(i) the symmetric coupling of the three cavities ($\rightarrow\rightarrow\rightarrow$), (ii) the symmetric coupling of the two external cavities, anti-symmetric to the central one whose dipole momentum is twice larger ($\rightarrow\longleftarrow\rightarrow$) and (iii) the anti-symmetric coupling of the external cavities leading to the extinction of the field in the central one ($\rightarrow 0 \leftarrow$). The calculated spectra are in good agreement with the measurements even though small shifts of the peaks may be noticed. These are attributed to the trapezoidal shape of the fabricated grooves while rectangular ones with perfectly conducting vertical walls are considered in the model. To account for this, effective heights had to be considered in the calculations ($h_{<1/1>} = 0.65$, $h_{<1/2>} = 0.7$ and $h_{<2/3>} = 0.59\ \mu m$). Moreover, the values of the widths at the top of the grooves ($w = 0.52$, 0.6 and 0.62 μm for gratings $< 1/1 >$, $< 1/2 >$ and $< 2/3 >$ respectively) and the nominal values of L and S, which are well defined by the fabrication process, were used.

To highlight the symmetric or anti-symmetric nature of the two sharp resonances of the $< 2/3 >$ grating, we have performed reflectivity measurements at various angles as increasing θ breaks the symmetry of the system and favors the excitation of the anti-symmetric. On the contrary the latter vanishes at normal incidence (the incident field is then symmetric and cannot couple with it)[24]. Experimental and calculated confirmations of this point are presented in figure 5 where the turnaround of the strength of the two resonances as a function of the incidence angle

#102049 - $15.00 USD Received 26 Sep 2008; revised 7 Oct 2008; accepted 12 Oct 2008; published 4 Nov 2008

is evidenced. It demonstrates that the peak at the smaller wave number is the anti-symmetric mode ($\rightarrow 0 \leftarrow$): it is weakly excited at small incidence angles and grows to become predominant around $\theta = 24^\circ$. This is confirmed by the maps of the intensity of the electric field along the x-axis above one period of the grating (Fig. 5(d)). The near-field distribution calculated at the resonance frequency of the antisymmetric mode ($\rightarrow 0 \leftarrow$) shows that the field localizes essentially in the grooves 1 and 3 while groove 2 is nearly extinguished. In contrast the field distribution of the symmetric mode ($\rightarrow\leftarrow\!\!-\!\!-\rightarrow$) is mainly located inside cavity 2 even though it stands at a strongly sub-wavelength distance from the neighboring cavities. By slightly changing the incident wavelength a spatial control of the hot spots can thus be performed and a new kind of light addressing in a chain of sub-wavelength resonator can be realized.

4. Conclusion

We have performed a study of the light localization inside deep sub-wavelength metallic grooves in commensurate gratings tending progressively to incommensurate structures. We theoretically demonstrate how these systems permit to generate, in a controlled manner, weakly radiative modes which localize strong and wavelength-dependant electromagnetic fields inside the grooves. These hot spots have the same behaviour than those commonly admitted to occur on disordered and/or SERS surfaces. Moreover we show that we can tune and spatially control, from far-field and at a sub-wavelength scale, the hot spots that may move from one cavity to another by slightly changing the incidence wavelength. Finally we gave an experimental evidence of these new modes via reflectivity measurements in the infra-red region and for two simple commensurate structures. Their existence demonstrates the validity of the theoretical approach and the possibility of applying it for experimental and applicative purposes.

#102049 - $15.00 USD Received 26 Sep 2008; revised 7 Oct 2008; accepted 12 Oct 2008; published 4 Nov 2008